Advances in Science and Technology Research Journal

Advances in Science and Technology Research Journal 2024, 18(2), 71–77
https://doi.org/10.12913/22998624/183949
ISSN 2299-8624, License CC-BY 4.0

Received: 2024.01.06
Accepted: 2024.02.15
Published: 2024.03.15

Characterization of the Mechanical Behavior of Hemp-Clay Composites

Chaimae Haboubi[1], El Hassane Barhdadi[1], Khadija Haboubi[1], Yahya El Hammoudani[1*], Zouhair Sadoune[2], Aouatif El Abdouni[1], Fouad Dimane[1]

[1] National School of Applied Sciences of Al-Hoceima, Department of Energy and Environmental Civil Engineering, Engineering Sciences and Applications Laboratory, Abdelmalek Essaâdi University, Tetouan, Morocco

[2] Department of Physics, Faculty of Science, Ibn Tofail University Kenitra, Morocco

* Corresponding author's e-mail: elhammoudani5@gmail.com

ABSTRACT

In the present study, micromechanical modeling techniques were employed to examine the mechanical properties of a hemp/clay composite material. This composite consists of hemp fibers incorporated into a clay matrix, a configuration chosen in response to environmental considerations and the natural advantages of hemp fibers, which include their lightweight nature and their considerable strength and stiffness relative to their weight. The approach adopted incorporates both localization and homogenization methodologies along with the three-phase model to provide an in-depth analysis of the composite's behavior. The findings from this theoretical model show a promising correlation with empirical data, demonstrating the model's efficacy in capturing the composite's mechanical response.

Keywords: hemp, clay, composite, micromechanical modeling, three-phase model.

INTRODUCTION

Derived from the Cannabis sativa plant, hemp fibers are a type of natural fiber. Cultivated legally in various countries, hemp finds usage across multiple sectors, including the production of paper, textiles, apparel, biodegradable plastics, construction materials, cosmetic items, health foods, and biofuels. The growth cycle of hemp, from seeding to full growth, spans roughly 12–16 weeks. Its significance as a natural fiber in industrial use is notable. Wang [1-3] highlights hemp's robust tensile strength and its effective resistance in alkaline conditions, making it an excellent reinforcing agent. Additionally, the hemp clay composite, a blend of ground clay bricks and organic binders, is recognized as a sustainable, eco-friendly material [4, 5].

Clay reinforced with hemp fiber presents numerous advantages, including its renewable nature and contribution to carbon sequestration [1, 6, 7]. This composite exhibits an impressive specific modulus, and understanding its properties is crucial for its effective application. These fiber-reinforced composites are categorized as hierarchical materials, featuring two levels of structure: the micro-scale and the macro-scale. The micro-scaale focuses on how particles are arranged within the matrix, while the macro-scale addresses the overall structural response of the material in engineering applications [6, 8]. For comprehensive multi-scale simulations of such composite materials, micro-scale techniques, which include both analytical and numerical methods, are typically employed. These methods are instrumental in estimating the composite's effective stiffness and strength, as well as its isotropic constitutive properties, thus providing a theoretical foundation for the design of engineering structures.

In the field of micromechanical analysis, the hemp/clay composite is typically studied through a representative volume element (RVE). This involves analyzing the RVE by applying conditions of displacement and traction continuity at the interfaces within and between elements, along with ensuring equilibrium conditions.

There are various micromechanics theories detailed in scholarly texts. A notable one is the Voigt model [9, 10], a relatively straightforward approach for forecasting the effective properties of a composite, initially devised for calculating average elastic constants in polycrystals. Conversely, the Reuss approximation [11, 12] is seen as the antithesis of the Voigt model [9]. Theoretical bounds on composite materials were set by Hashin [13] and further developed in the Hashin-Shtrikman [14] framework. Eshelby [15] tackled the issue of ellipsoidal inclusions within an infinite isotropic matrix. Additionally, the Mori-Tanaka method [16] was introduced to assess the average internal stress in matrices containing precipitates with inherent strains.

In addition to the composite's mechanical properties and simulation methodologies, it is crucial to delve into the holistic attributes of the hemp fiber-reinforced clay composite, focusing on its durability and how external environmental factors impact its performance. The comprehensive properties of this composite material underscore its robustness and long-term stability under various conditions. Durability studies indicate that hemp fiber reinforcement significantly enhances the composite's resistance to physical and chemical degradation over time, thereby extending its lifespan. Factors such as moisture, temperature fluctuations, and UV exposure have been systematically evaluated to understand their effects on the composite's integrity. Hemp fibers exhibit a notable resilience against moisture absorption, which mitigates the risk of mold growth and material breakdown, a common concern in bio-based materials. Thermal analysis reveals that the composite maintains its structural integrity across a wide temperature range, showcasing its suitability for diverse climatic conditions. Additionally, the impact of UV radiation has been studied, with findings suggesting that the surface treatment of hemp fibers can effectively reduce UV-induced degradation, thereby preserving the material's mechanical properties and appearance. This holistic understanding of the material's properties not only highlights its environmental adaptability but also its potential for applications requiring long-term durability and resilience to external factors.

The foundational concept of the composite fiber model has been and continues to be a cornerstone in the development of numerous micromechanical models. Hashin [13] pioneered this field with the introduction of the composite spheres model. Building on this, Christensen [17] expanded the theory to encompass composite materials with ellipsoidal inclusions. Furthering this adaptation, Christensen and Lo [18] modified the model to apply to composites with cylindrical reinforcements.

In our study, we concentrate on calculating the effective material characteristics of unidirectional hemp fiber-reinforced clay, employing a three-phase model [17]. This model incorporates a design featuring cylindrical hemp inclusions and a cylindrical clay matrix layer, combined within an equivalent homogeneous medium. This configuration effectively represents a two-phase composite of Fiber and Matrix. Our analytical approach to this model assumes several conditions: all components are linear, elastic, and isotropic; there is a flawless bond between the fiber and the matrix; the fibers are continuous, parallel, and evenly dispersed within the matrix; the composite material is devoid of any voids; and the elasticity, diameters, and spacing of the fibers are consistent throughout.

GENERAL FRAMEWORK

Figure 1 is a schematic representing a hemp/clay composite material. In materials science, diagrams like this are used to illustrate the microstructure or composition of composite materials.

Two types of composite fibers of different sizes that make up the hemp/clay composite material. In such composites, fibers (hemp, in this case) are embedded within a matrix (clay) to enhance material properties such as strength, durability, and rigidity. Composite materials are engineered by combining two or more constituent materials with significantly different physical or chemical properties. In the case of hemp/clay composites, the aim is often to create a material that is sustainable, environmentally friendly, and has good mechanical properties.

Following Christensen and Lo [17], except for one individual composite fiber, all others composites fibers are replaced by the equivalent

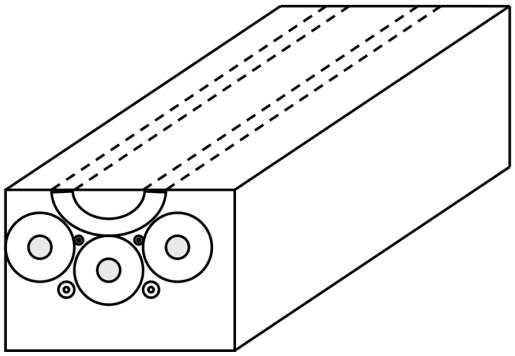

Fig. 1. The schematization of the two-composite fiber model

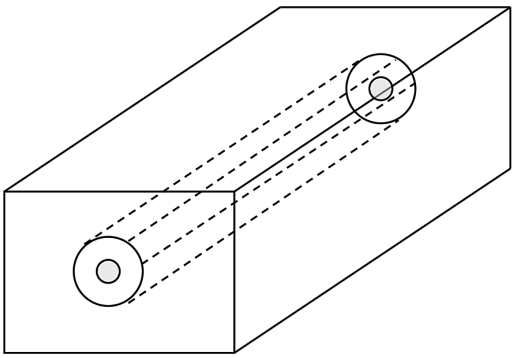

Fig. 2. The three-phase model

homogeneous medium with unknown properties. Figure 2 provides a three-phase model for a hemp/clay composite material, emphasizing the structural and interactional aspects of the composite. The central feature, a cylinder with a concentric inner circle, represents a hemp fiber with a distinct core-shell morphology. This dual structure is indicative of the complex internal composition of hemp fibers, which can possess different mechanical properties in their core and outer layers, affecting the overall performance of the composite. The surrounding dashed lines suggest the clay matrix phase, enveloping the hemp fiber. These lines may symbolize the matrix's continuity and its mechanical interplay with the embedded fiber, a critical factor in the load distribution and stress handling of the composite.

Adjacent to the main representation is a small, separate circle, whose role within the model is less clear but could denote a third phase or a point of interest within the composite system. It could symbolize a distinct inclusion, such as a particulate filler or a pore within the matrix, which could have implications for the material's properties, such as density or thermal behavior. Overall, this diagram abstracts the essential elements of the hemp/clay composite into a simplified form, facilitating the understanding of its microstructure and the synergistic effects that govern its mechanical attributes. The model underscores the importance of each phase and their interactions, which are fundamental to the design and optimization of composite materials for desired applications.

In the conceptualized model depicted in Figure 2, the fibers are modeled as continuous, cylindrical entities with a circular cross-section, systematically arranged in a periodic pattern. The composite structure is conceptualized as consisting of repeating cylindrical unit cells or Representative Volume Elements (RVEs). As illustrated in Figure 2, each RVE is constituted of a central cylindrical hemp fiber with a radius denoted by "a," which is encased within a concentric hollow clay matrix cylinder with a larger radius "b." The volume fraction of the hemp fibers within the composite is determined using the ratio $V_f = a^2/b^2$, which represents the square of the ratio of the fiber radius to the matrix radius.

Over the representative volume element, the averages of internal strain and stress fields denoted by E and Σ are given by:

$$\Sigma = f_1\sigma^1 + f_2\sigma^2 \, , E = f_1\varepsilon^1 + f_2\varepsilon^2 \qquad (1)$$

The subscripts 1 and 2 denote fiber and matrix, respectively.

These averages serve to define the effective elastic stiffness of the composite C^{eff} according to the relation:

$$\Sigma = C^{eff} : E \qquad (2)$$

f_1 and f_2 indicate the volume fractions of the hemp fiber and the clay matrix layer, respectively, such that:

$$f_1 + f_2 = 1 \qquad (3)$$

The average stress σ^i, and the average strain ε^i, in phase, i (i =1, 2) are given by:

$$\sigma^i = \frac{1}{V_i}\int_{V_i} \sigma\,(x)dV \, , \; \varepsilon^i = \frac{1}{V_i}\int_{V_i} \varepsilon(x)dV \qquad (4)$$

V_i is the volume of phase i and the constitutive equations relating the average stress and strain of the inclusion and the matrix layer are respectively:

$$\sigma^1 = c^1 : \varepsilon^1 \, , \sigma^2 = c^2 : \varepsilon^2 \qquad (5)$$

The constitutive and field equations of elasticity authorize the introduction of the strain concentration tensors A^1 and A^2 such that:

$$\varepsilon^1 = A^1 : E \, , \varepsilon^2 = A^2 : E \qquad (6)$$

Using the foregoing equations, one can express the effective properties that requires the estimation of the strain localization tensor :

$$C^{eff} = c^2 + f_1(c^1 - c^2): A^1 \tag{7}$$

With c^1 and c^2 are the stiffness matrices of the matrix phase and the reinforcement phase (fibers) respectively. A^1 is the strain concentration tensor deduced from the Eshelby tensor and given by:

$$A^1 = [I + T: (c^2)^{-1}: (c^1 - c^2)]^{-1} \tag{8}$$

With I is the unit tensor and T is the Eshelby tensor which depends on the shape of the inclusion and the Poisson's ratio of the matrix. More detailed information about the Eshelby tensor could be found in Mura [19]. The Eshelby tensor is then calculated for each inclusion along with the stiffness matrix. Using Christensen et al. [17], one can obtain the five elastic constants of fiber/matrix composite by applying proper boundary conditions to the RVE as follows:

- Longitudinal elastic modulus.

Assuming the composite is subjected to axial loading in the fiber direction, the longitudinal elastic modulus is obtained by:

$$E_L = fE_1 + (1-f)E_2 + \frac{f(1-f)(\nu_1 - \nu_2)^2}{\frac{f}{\kappa_1} + \frac{1}{\mu_2} + \frac{1-f}{\kappa_1}} \tag{9}$$

- Poisson's ratio.

$$\nu = f\nu_1 + (1-f)\nu_2 + \frac{f(1-f)(\nu_1 - \nu_2)(1/\kappa_2 - 1/\kappa_1)}{\frac{f}{\kappa_1} + \frac{1}{\mu_2} + \frac{1-f}{\kappa_1}} \tag{10}$$

- Longitudinal shear modulus.

$$\mu_L = \mu_2 \frac{\mu_1(1+f) + \mu_2(1-f)}{\mu_1(1-f) + \mu_2(1+f)} \tag{11}$$

- Bulk modulus.

$$\kappa_L = \kappa_2 + \frac{f}{\frac{1}{\kappa_1 - \kappa_2} + \frac{1-f}{\kappa_2 + \mu_2}} \tag{12}$$

- Transverse shear modulus.

$$\mu_T = \mu_2 + \frac{f\mu_2}{\frac{\mu_2}{\mu_1 - \mu_2} + \frac{(1-f)(\kappa_2 + 2\mu_2)}{2\kappa_2 + 2\mu_2}} \tag{13}$$

Hashin and Shtrikman propose a tighter bounding of the properties of a multiphase material than Voigt and Reuss. Additionally, this model adds an extra assumption about the geometry, namely the existence of two phases, one being continuous and the other discontinuous [20].

This model uses the variational principle: the various constituents are embedded in a reference material. If the reference material is stiffer, we find the upper bound of the composite's rigidity; however, if the reference material is more flexible, we reach the lower bound of the composite's rigidity [21].

The equations defining the lower and upper bounds of the effective compression modulus denoted as KHS, and the effective shear modulus, denoted as GHS, are as follows [22]:

$$K^{HS} = \left((1-f)K_m + fK_f\right) - \frac{f(1-f)(K_m - K_f)^2}{(1-f)K_f + fK_m + \tilde{K}} \tag{14}$$

with:

$\tilde{K} = max\left\{\frac{4}{3}G_m; \frac{4}{3}G_f\right\}$ – for the upper bound,

$\tilde{K} = min\left\{\frac{4}{3}G_m; \frac{4}{3}G_f\right\}$ – for the lower bound.

$$G^{HS} = \left((1-f)G_m + fG_f\right) - \frac{f(1-f)(G_m - G_f)^2}{(1-f)G_f + fG_m + \tilde{G}} \tag{15}$$

with:

$\tilde{G} = max\left\{\frac{G_m(9K_m + 8G_m)}{6(K_m + 2G_m)}; \frac{G_f(9K_f + 8G_f)}{6(K_f + 2G_f)}\right\}$ – for the upper bound,

$\tilde{G} = min\left\{\frac{G_m(9K_m + 8G_m)}{6(K_m + 2G_m)}; \frac{G_f(9K_f + 8G_f)}{6(K_f + 2G_f)}\right\}$ – for the lower bound.

These two modules are related to Young's modulus and Poisson's ratio through these relationships of isotropic elasticity:

$$G = \frac{E}{2(1+\nu)} \; and \; K = \frac{E}{3(1-2\nu)} \; and \; E = \frac{9KG}{3G+K}$$

Subsequently, one can deduce the expression of Young's modulus using the laws of isotropic elasticity through these two formulas:

– for the lower bound:

$$E^{HS+} = \left(f K_f + \frac{(1-f)E_m}{1 + \alpha_f \frac{E_m - E_f}{E_f}}\right)\left(f + \frac{(1-f)}{1 + \alpha_f \frac{E_m - E_f}{E_f}}\right)^{-1}$$

– for the upper bound :

$$^{HS-} = \left((1-f)E_m + \frac{f E_f}{1 + \beta_m \frac{E_f - E_m}{E_m}}\right)\left(1 - f + \frac{f}{1 + \beta_m \frac{E_f - E_m}{E_m}}\right)^{-1}$$

RESULTS AND DISCUSSIONS

Figure 3 depicts the relationship between the volume fraction of hemp fibers and the effective shear modulus of the hemp/clay composite material. The horizontal axis represents the independent variable, typically a parameter of interest in the study such as time, temperature, or applied load. For mechanical behavior characterization, this could be strain or stress levels applied to the hemp/clay composite. The vertical axis denotes the dependent variable, which is the response measured during the experiment or simulation. In the context of mechanical behavior, this is often a measure of strength, stiffness, or deformation, such as stress, modulus, or strain, respectively.

The graph presents a curve that reflects the increasing trend of the composite's shear modulus with an increasing proportion of hemp fibers in the clay matrix. This trend is consistent with the reinforcing effect expected when high-modulus fibers are added to a lower-modulus matrix. The predicted values are juxtaposed with the theoretical bounds provided by the Hashin-Shtrikman models, referenced as [8] in the document. The upper and lower bounds of the Hashin-Shtrikman models represent the theoretical maximum and minimum shear moduli the composite could achieve under idealized conditions, taking into account the shear moduli and Poisson's ratios of both phases: the hemp fiber (μ_1 = 28.5 GPa, ν_1 = 0.23) and the clay matrix (μ_2 = 1.75 GPa, ν_2 = 0.4). These moduli values suggest a significant discrepancy in stiffness between the fiber and matrix, which is a characteristic feature in fiber-reinforced composites aimed at enhancing strength and stiffness. The graph illustrates that the actual effective shear modulus of the composite lies within the Hashin-Shtrikman bounds, indicating that the model is a good predictor of the composite's behavior. The convergence of experimental data towards the upper bound as the fiber volume fraction increases suggests that the fibers' contribution to the composite's shear strength is maximized at higher fiber concentrations.

Figure 4 presents the experimentally measured effective Young's modulus of a hemp/clay composite material as a function of the hemp fiber volume fraction. The data points, represented by the blue dots, illustrate the modulus behavior in relation to the increasing presence of hemp within the composite. Accompanying the experimental data is a fitted curve that is likely derived from the present model being discussed in the study. This model is expected to predict the composite's stiffness based on the individual stiffness values of the hemp fibers and the clay matrix, as well as their respective Poisson's ratios.

The mechanical properties of the constituents – namely the Young's modulus $V_2 = 1.75E_2$ = 1.75 GPa with a Poisson's ratio $V_2 = 0.4\nu_2$ = 0.4 for the clay matrix, and $V_1 = 28.5E_1 = 28.5$ GPa with a Poisson's ratio $V_1 = 0.23\nu_1 = 0.23$ for the hemp fibers-highlight the disparity between the stiffness of the matrix and the reinforcing fibers. The anticipated increase in stiffness with a higher volume fraction of reinforcement

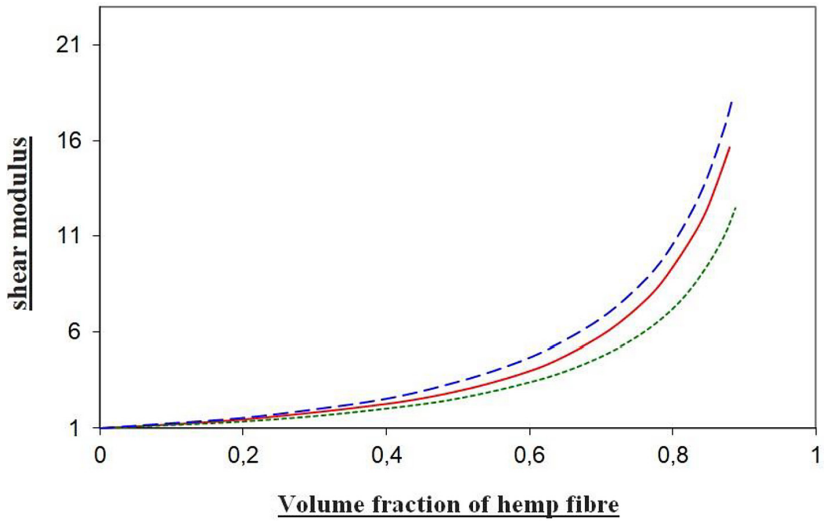

Fig. 3. Normalized effective shear modulus (μ_{eff}/μ_2) versus the volume fraction of hemp fiber: red line = present model, dotted blue (blue)/green line = upper/lower Hashi-Shtrikman bound

is not observed; rather, the effective Young's modulus shows a downward trend. This suggests that factors beyond the Young's modulus of individual components are influencing the composite's overall stiffness. Numerical predictions indicate that while individual hemp fibers have a Young's modulus of 28.5 GPa, and the clay matrix a much lower 1.75 GPa, the interaction between these two phases does not result in a straightforward additive increase in stiffness. The composite's effective Young's modulus, a quantifiable measure of the combined stiffness, is expected to reflect the synergistic effects of the fiber-matrix interface quality and the distribution and concentration of fibers. For instance, a hypothetical numerical model might predict that an increase in fiber volume fraction from 10% to 20% would ideally enhance the composite's modulus by a certain percentage, provided the fiber dispersion remains uniform and the interfacial bond remains strong. However, due to potential factors such as fiber agglomeration or suboptimal interfacial adhesion, the actual increase in stiffness may deviate from this prediction, which necessitates a detailed investigation into these contributing issues.

Figure 4 is a graph of the Young's modulus (E_1) against the volume fraction of hemp fiber in the composite. The data points suggest that the Young's modulus, indicative of the material's stiffness, decreases as the volume fraction of hemp fiber increases. This is an intriguing trend since, intuitively, one might expect the stiffness to increase with a higher concentration of reinforcing fibers. Typically, the inclusion of fibers like hemp is intended to enhance the composite's rigidity.

However, the downward trajectory of the curve in Figure 4 implies that the composite may not be benefiting from the added fibers beyond a certain concentration. This could be due to several factors. For instance, at higher fiber concentrations, the fibers may begin to agglomerate, creating points of weakness rather than providing uniform reinforcement. Another possibility is that the interface between the hemp fibers and the clay matrix may not be strong enough to effectively transfer loads, especially as the fiber content increases.

The curve in the graph represents a predictive model that fits the experimental data, possibly derived from a theoretical approach such as a rule of mixtures, which is often used to predict the overall properties of a composite material based on its constituents. The discrepancy between the expected and observed trends could highlight the need for a more nuanced model that accounts for the complex interactions between fiber and matrix at various concentrations. It also suggests that there is an optimal fiber volume fraction where the composite achieves maximum stiffness, after which the effectiveness of fiber reinforcement diminishes. Further investigations into the fiber-matrix interface, fiber alignment, distribution, and potential chemical modifications could provide more insights and lead to an improved composite design.

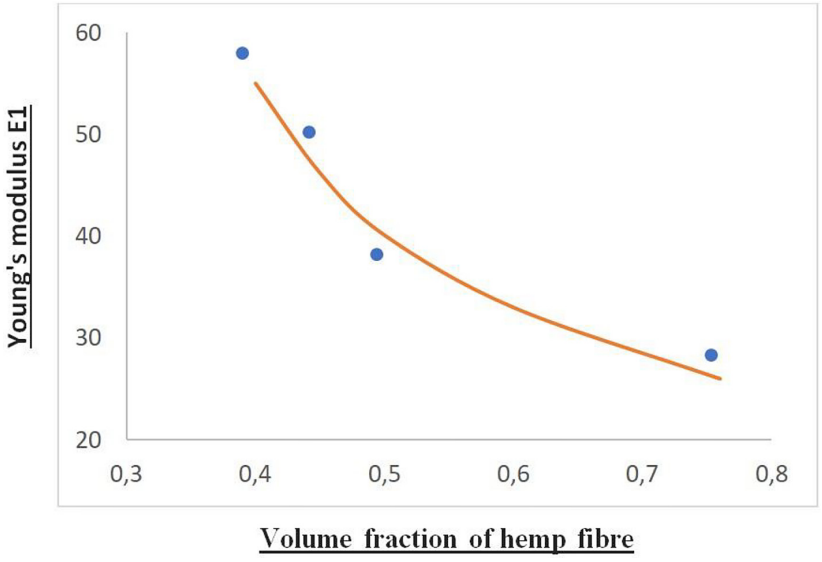

Figure 4. Effective Young's modulus (MPa) of hemp/clay composite against volume fraction of hemp

CONCLUSIONS

In this work, a micromechanical approach to estimate the effective elastic properties of a two-phase composite with cylindrical reinforcements and perfect bonding has been developed. Analytical formulations are obtained using the localization method, homogenization method, and on the three-phase model. The Eshelby inclusion problem with a perfect interface is used in the case of displacement and traction continuities across the interface and the obtained effective properties require only the estimation of the strain localization tensor in inclusion. Christensen and Lo's model was applied to estimate the effective elastic moduli of composites with cylindrical reinforcements and perfect bonding.

It is shown that with the obtained analytical results, one can evaluate the overall elastic properties of a real two-phase composite made of hemp fiber embedded in a clay matrix. The results of the present model are compared successfully with experimental data. The calculated Young's modulus is close to the test result for all ranges of fiber content, suggesting that the present model is suitable for the elastic modulus estimation of fiber-reinforced composites.

REFERENCES

1. Collet F., Pretot S. Experimental investigation of moisture buffering capacity of sprayed hemp concrete. Construction and Building Materials 2012; 36(3): 58–65.
2. Ait Mansour A., El-Haitout B., Adnin R.J., Lgaz H., Salghi R., Lee H.-S., Alhadeethi M.R., Messali M., Haboubi K., Ali I.H. Insights into the Corrosion Inhibition Performance of Isonicotinohydrazide Derivatives for N80 Steel in 15% HCl Medium: An Experimental and Molecular Level Characterization. Metals 2023; 13(4): 797.
3. Elabdouni A., Haboubi K., Bensitel N., Bouhout S., Aberkani K., El Youbi M.S. Removal of organic matter and polyphenols in the olive oil mill wastewater by coagulation-flocculation using aluminum sulfate and lime. Moroccan Journal of Chemistry 2022; 10(1): 191–202.
4. Gioffré M., Vincenzini A., Cavalagli N., Gusella V., Caponero M., Terenzi A., Pepi C. A novel hemp-fiber bio-composite material for strengthening of arched structures: Experimental investigation. Construction and Building Materials 2021; 308(124969).
5. Fernine Y., Arrousse N., Haldhar R., Raorane C.J., Kim S.-C., El Hajjaji F., Touhami M.E., Beniken M., Haboubi K., Taleb M. Synthesis and characterization of phenolphthalein derivatives, detailed theoretical DFT computation/molecular simulation, and prevention of AA2024-T3 corrosion in medium 3.5% NaCl. Journal of the Taiwan Institute of Chemical Engineers 2022; 140(104556).
6. Pretot S., Collet F., Garnier C., Life cycle assessment of a hemp concrete wall: Impact of thickness and coating. Building and Environment 2014; 72: 223–231.
7. Amziane S., Arnaud L. Bio-aggregate-based Building Materials 2013.
8. Andaloussi K., Achtak H., Nakhcha C., Haboubi K., Stitou M. Assessment of soil trace metal contamination of an uncontrolled landfill and its vicinity: the case of the city of 'Targuist'(Northern Morocco). Moroccan Journal of Chemistry 2021; 9(3): 9–3, 513–529.
9. Voigt W. Ueber die Beziehung zwischen den beiden Elasticitätsconstanten isotroper Körper. Annalen der Physik 1889; 274(12): 573–587.
10. Bouhout S., Haboubi K., El Abdouni A., El Hammoudani Y., Haboubi C., Dimane F., Hanafi I., Elyoubi M.S. Appraisal of Groundwater Quality Status in the Ghiss-Nekor Coastal Plain. Journal of Ecological Engineering 2023; 24(10).
11. Bumanis G., Vitola L., Pundiene I., Sinka M., Bajare D. Gypsum, geopolymers, and starch-alternative binders for bio-based building materials: A review and life-cycle assessment. Sustainability (Switzerland) 2020; 12(14).
12. Bourjila A., Dimane F., Ghalit M., Taher M., Kamari S., El Hammoudani Y., Achoukhi I., Haboubi K. Mapping the spatiotemporal evolution of seawater intrusion in the Moroccan coastal aquifer of Ghiss-Nekor using GIS-based modeling. Water Cycle 2023; 4: 104–119.
13. Hashin Z. The elastic moduli of heterogeneous materials. 1960: US Department of Commerce, Office of Technical Services.
14. Hashin Z., Shtrikman S. A variational approach to the theory of the elastic behaviour of multiphase materials. Journal of the Mechanics and Physics of Solids 1963; 11(2): 127–140.
15. Eshelby J.D. The determination of the elastic field of an ellipsoidal inclusion, and related problems. Proceedings of the royal society of London. Series A. Mathematical and Physical Sciences 1957; 241(1226): 376–396.
16. Mori T., Tanaka K. Average stress in matrix and average elastic energy of materials with misfitting inclusions. Acta metallurgica 1973; 21(5): 571–574.
17. Christensen R.M. A critical evaluation for a class of micro-mechanics models. Journal of the Mechanics and Physics of Solids 1990; 38(3): 379–404.
18. Christensen R., Lo K. Solutions for effective shear properties in three phase sphere and cylinder models. Journal of the Mechanics and Physics of Solids 1979; 27(4): 315–330.
19. Mura T. Micromechanics of defects in solids. 2013: Springer Science & Business Media.
20. Attard T.M., Goodwin C., Nalivaika P., Attard J., Budarin V.L., Lanot A., Bove D., Clark J.H., McElroy C.R. Simple, quick and green isolation of cannabinoids from complex natural product extracts using sustainable mesoporous materials (Starbon®). Materials Chemistry Frontiers 2022.
21. Böhm H.J. A short introduction to basic aspects of continuum micromechanics. Cdl-fmd report 1998; 3.
22. Frankowski J., Zaborowicz M., Sieracka D., Łochyńska M., Czeszak W, Prediction of the hemp yield using artificial intelligence methods. Journal of Natural Fibers 2022; 19(16): 13725–13735.